Supplementary material

NO/ROS/RNS Cascaded-Releasing Nano-Platform for Gas/PDT/PTT/Immunotherapy of Tumor

Mengchao Ding[a], Kai Shao[b], Lijuan Wu[c], Yuping Jiang[a], Bing Cheng[a], Lili Wang[d], Jinsheng Shi[a*], Xiaoying Kong[a*]

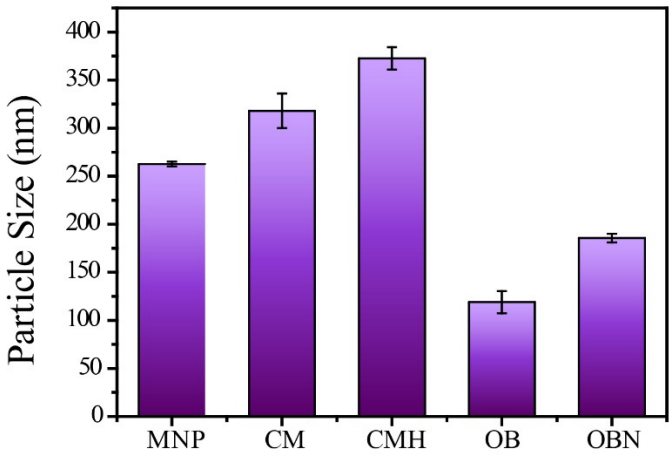

Figure S1. The particle size of MNP, CM, CMH, OB and OBN NPs.

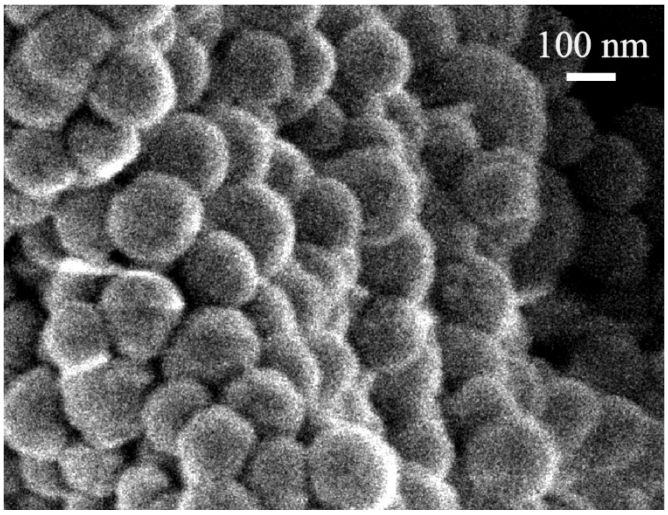

Figure S2. The SEM of CMH NPs.

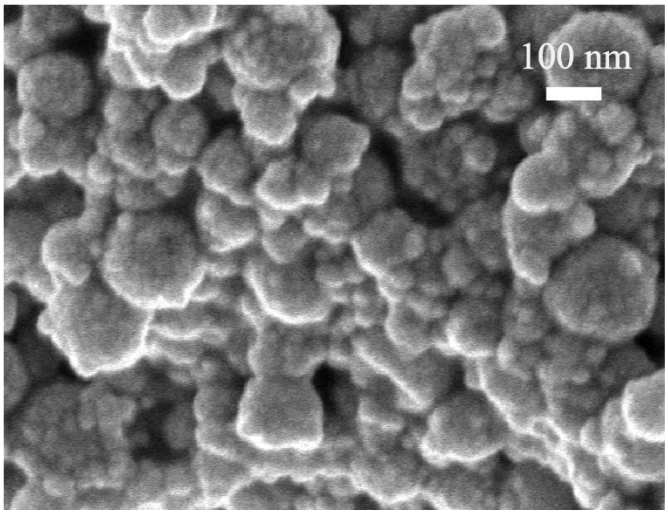

Figure S3. The SEM of OBN microcapsules.

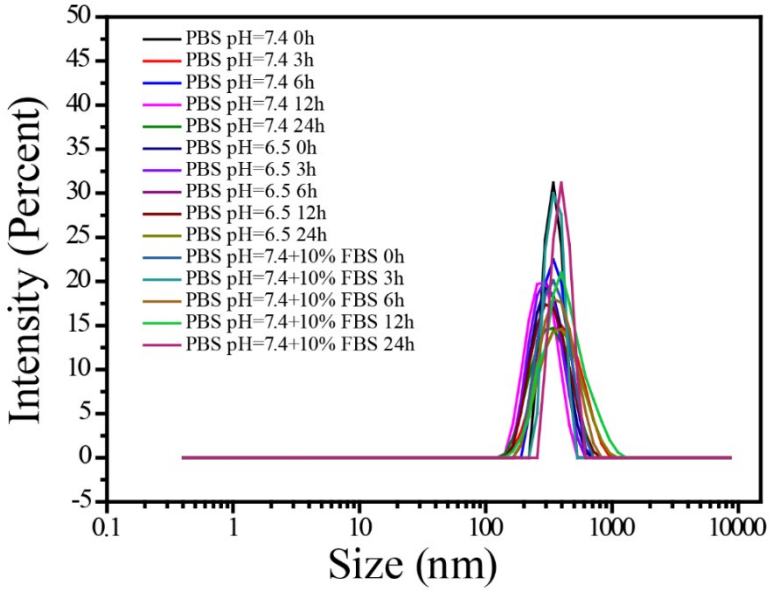

Figure S4. Stability of particle size of CMH in different simulation environments.

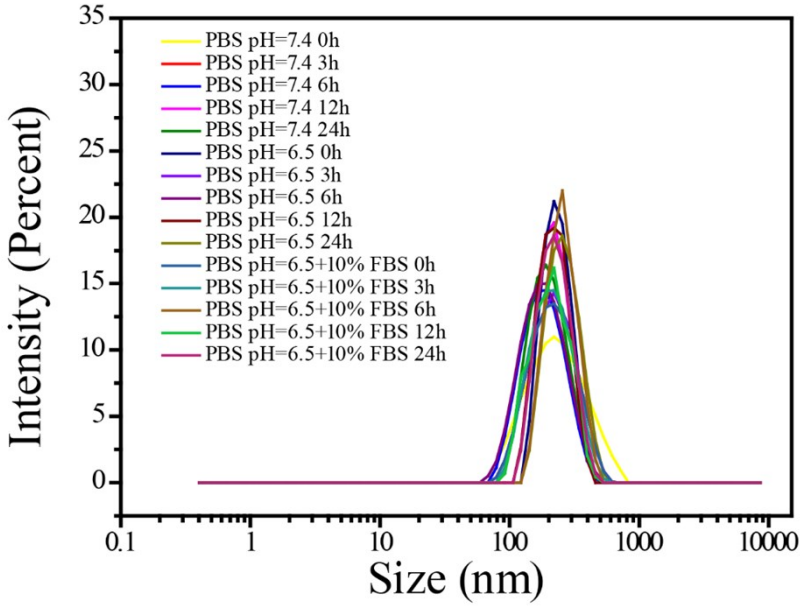

Figure S5. Stability of particle size of OBN in different simulation environments.

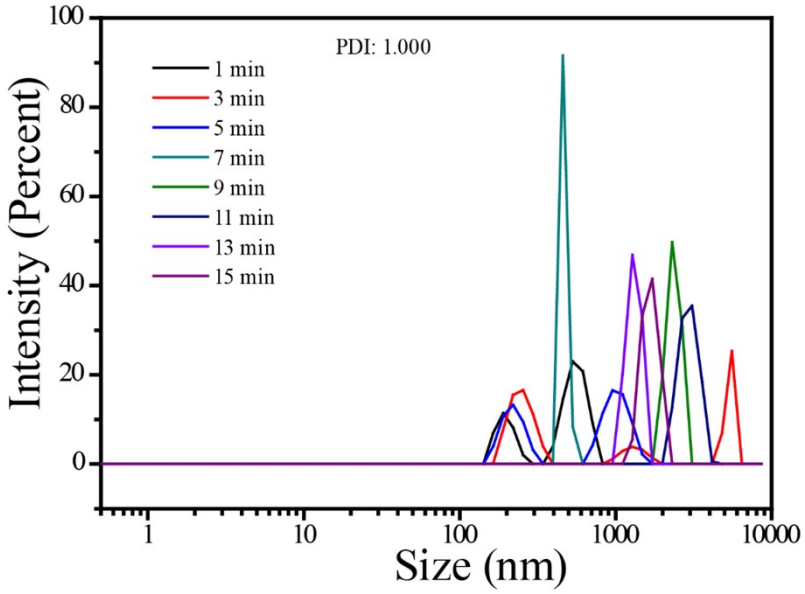

Figure S6. The change of size distribution of OBN microcapsules with ROS.

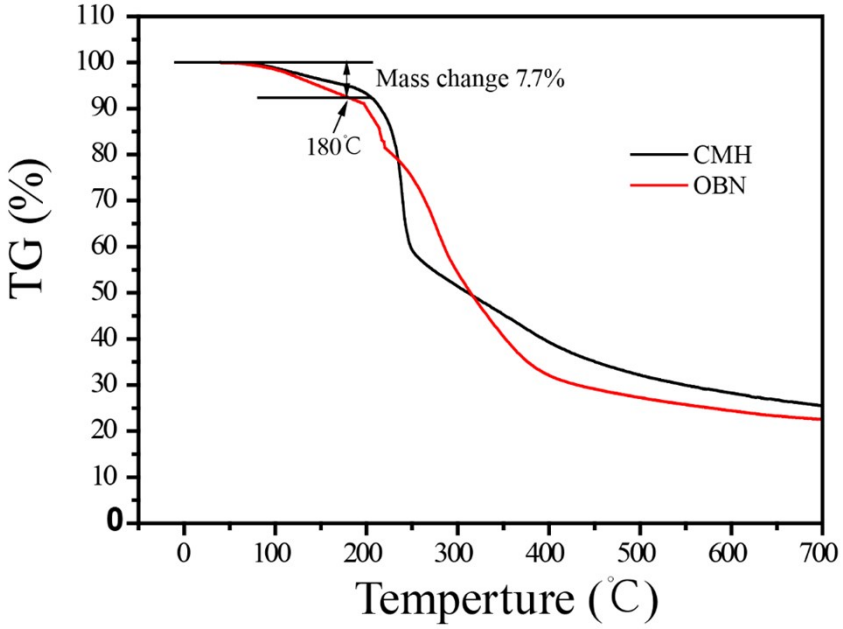

Figure S7. The TG curves of CMH NPs and OBN microcapsules.

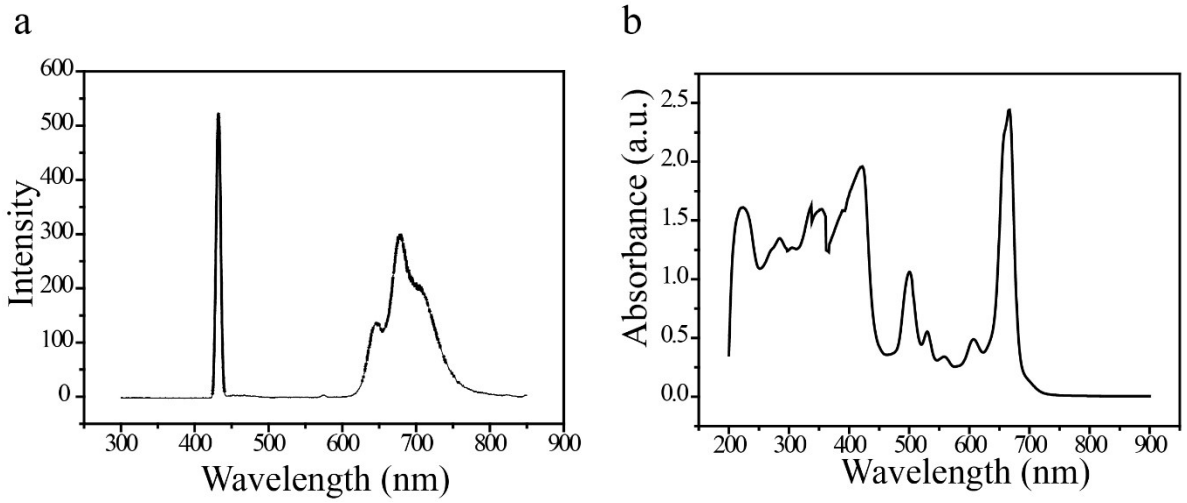

Figure S8. UV-vis-NIR absorption spectra (a) and Fluorescence excitation spectra (b) of Ce6.

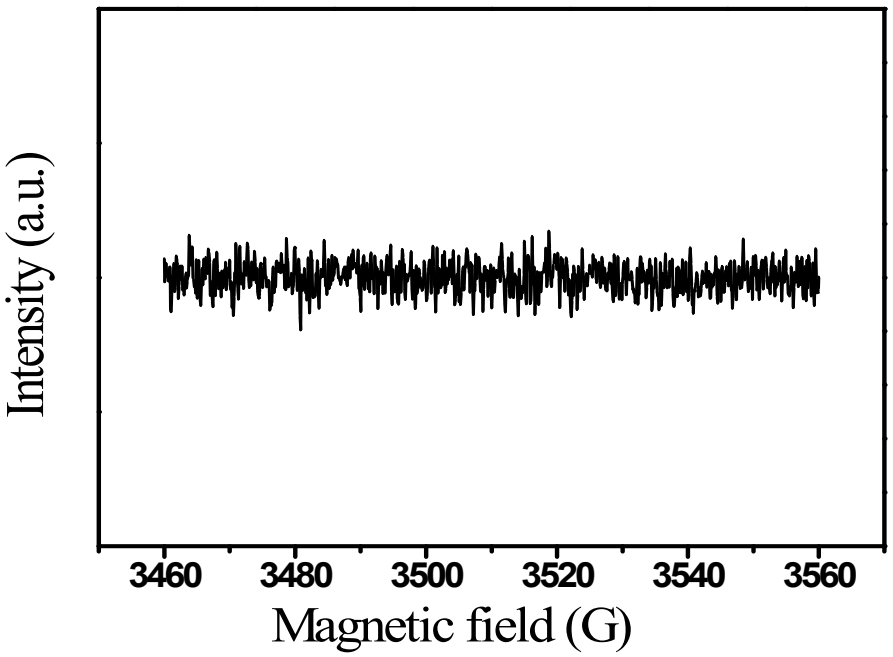

Figure S9. •OH EPR spectra of CMH NPs with 808 nm laser (1 W cm^{-2}, 5 min) and blank control group.

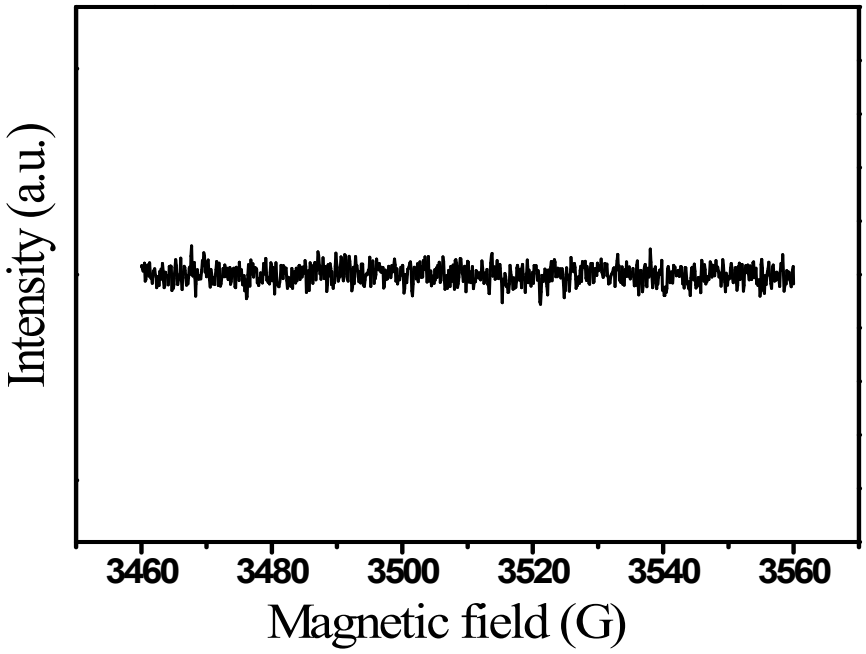

Figure S10. $O_2^{\bullet-}$ EPR spectra of CMH NPs with 808 nm laser (1 W cm^{-2}, 5 min) and blank.

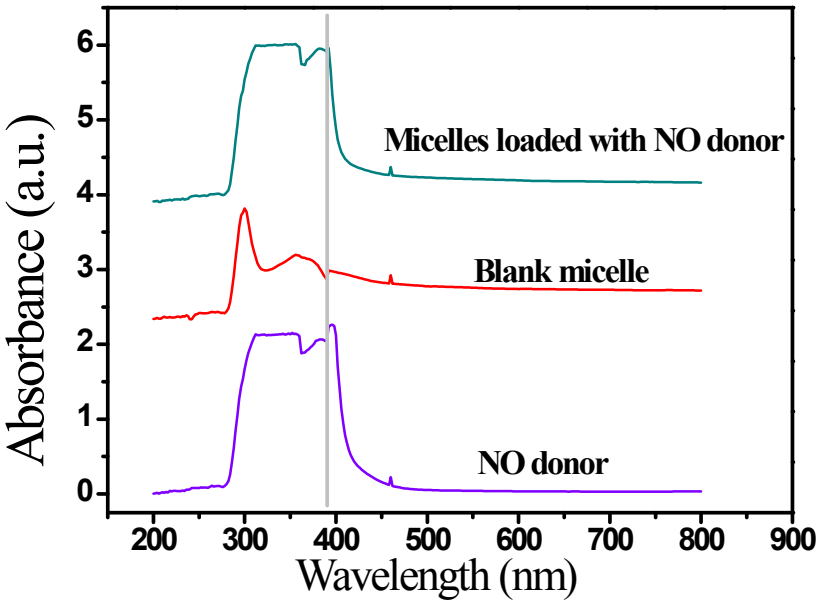

Figure S11. UV-vis-NIR absorption spectra of benzofuroxan (NO donor), OB micelle and OBN micelles.

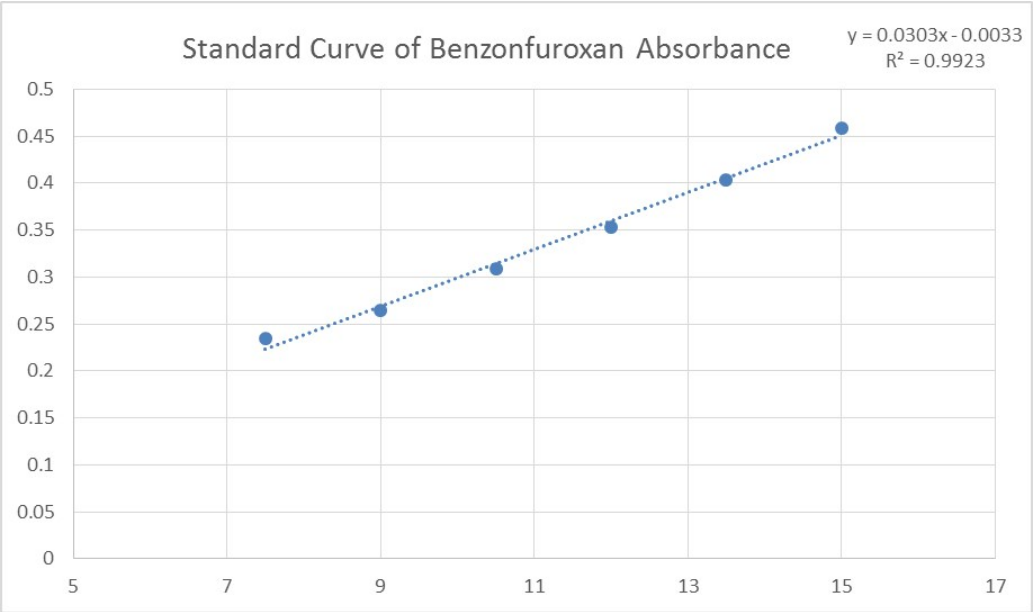

Figure S12. Standard curve of absorbance of benzonfuroxan.

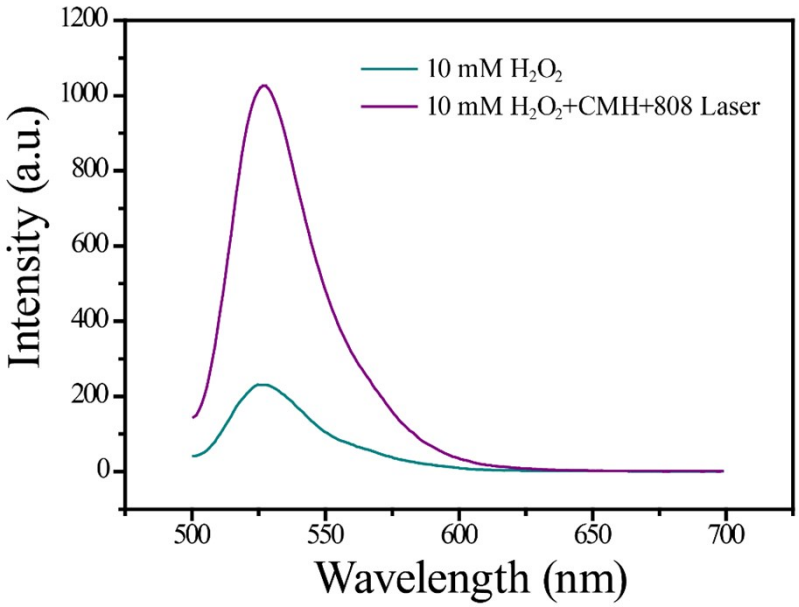

Figure S13. Fluorescence intensity of ROS of 10 mM H_2O_2 and 10 mM H_2O_2+ CMH NPs (1 mg mL^{-1}) under 808 nm laser irradiation (1 W cm^{-2}, 5 min).

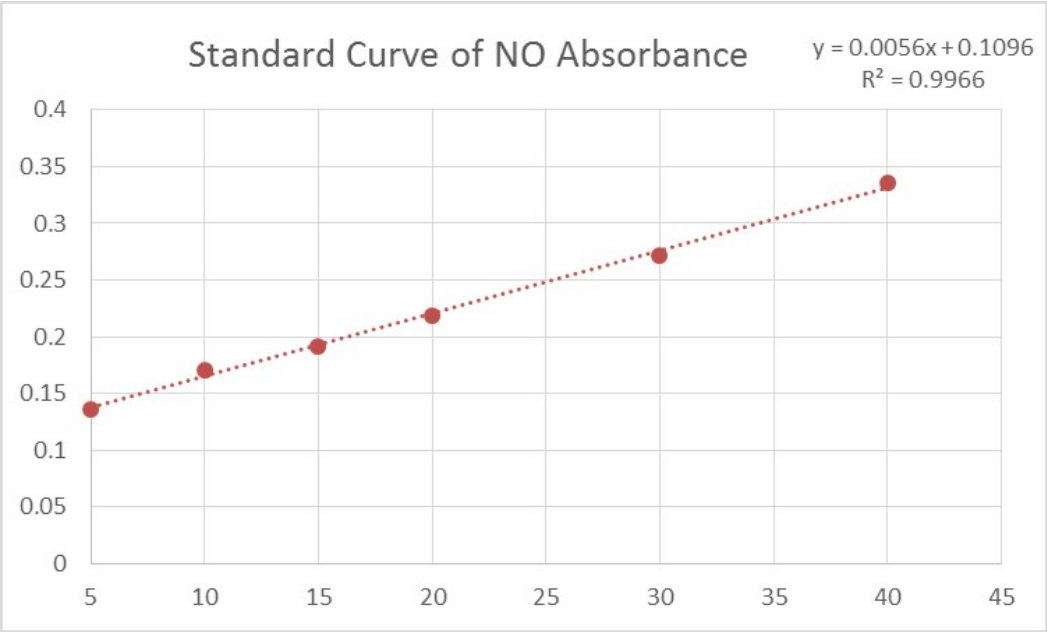

Figure S14. Standard curve of absorbance of NO.

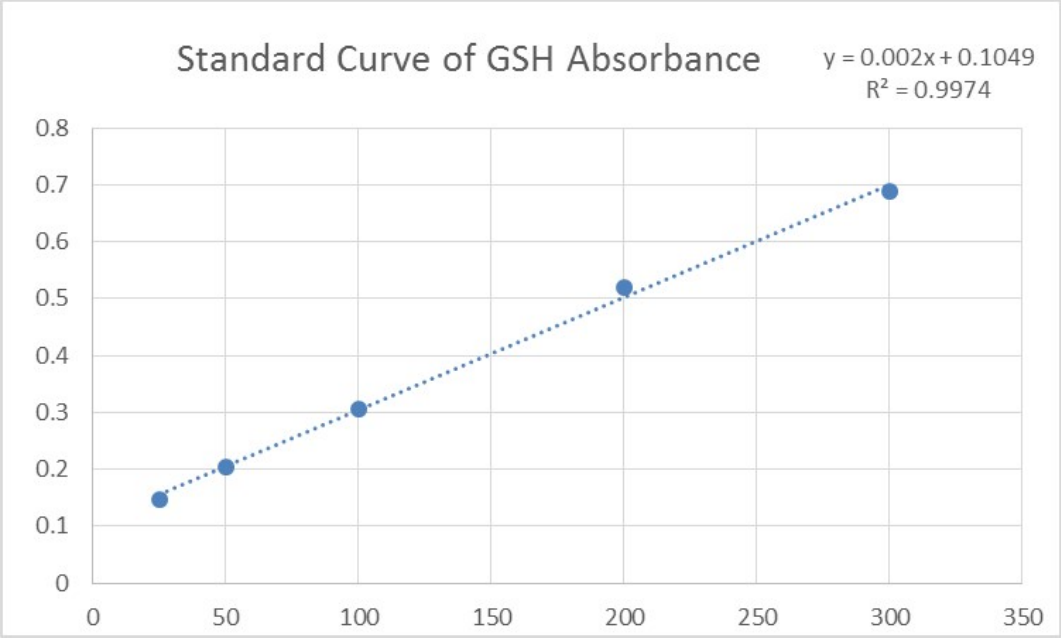

Figure S15. Standard curve of absorbance of GSH.

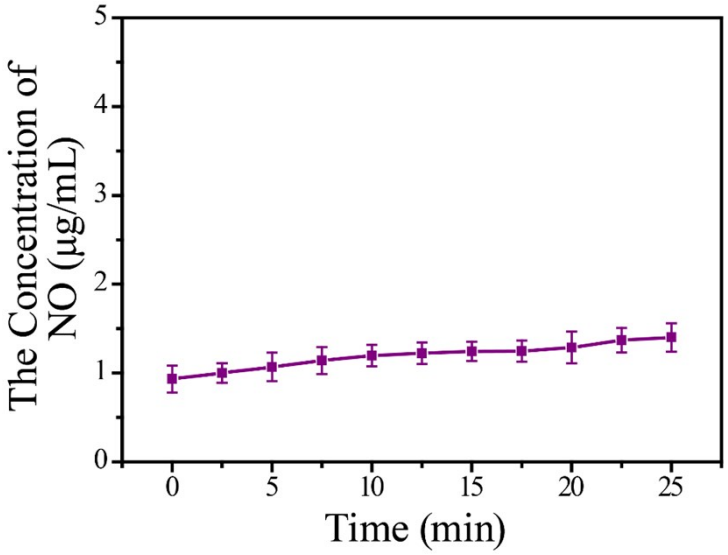

Figure S16. The amount of NO released in 2 mM GSH.

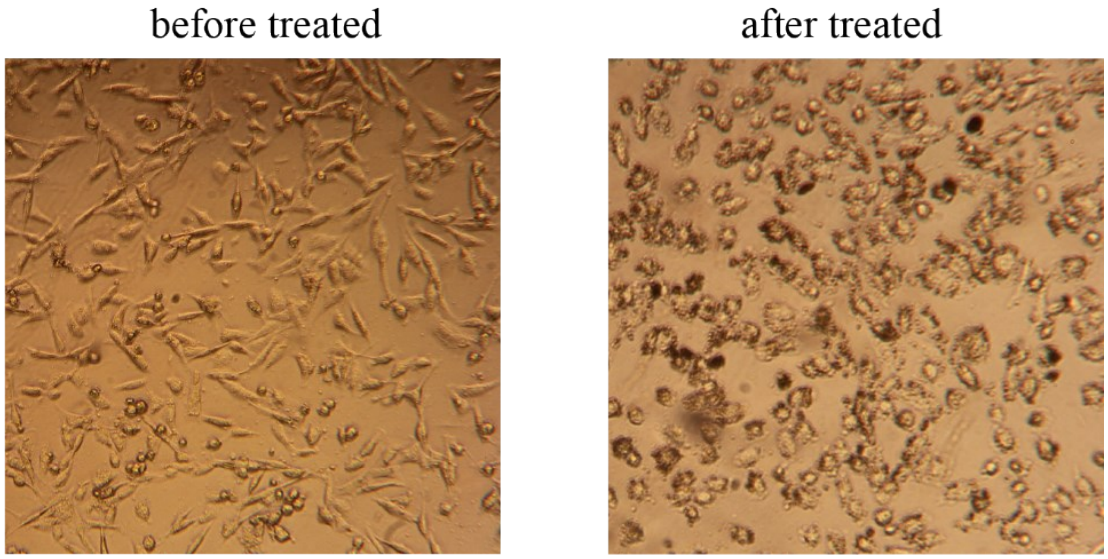

Figure S17. The cell morphology of 4T1 before and after treatment with CMH-OBN nano-platform under 808 nm irradiation (1 W cm^{-2}, 5 min).

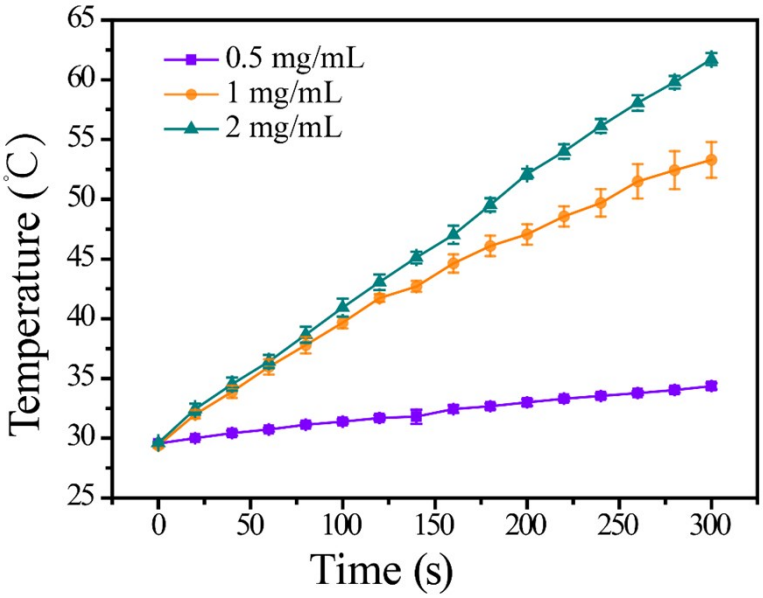

Figure S18. Temperature rise curves of CMH NPs with different concentrations upon irradiation (808 nm, 1 W cm^{-2}, 5 min).

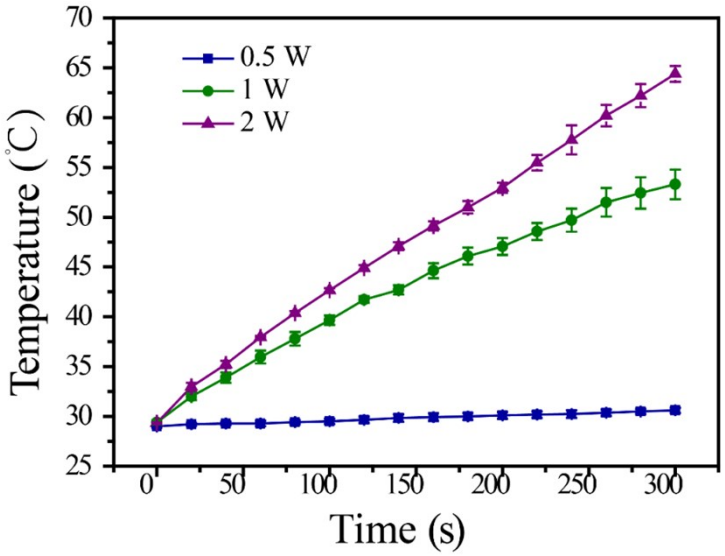

Figure S19. Temperature rise curves of CMH NPs with different wattage laser irradiation irradiation (808 nm, 1 mg mL^{-1}, 5 min).

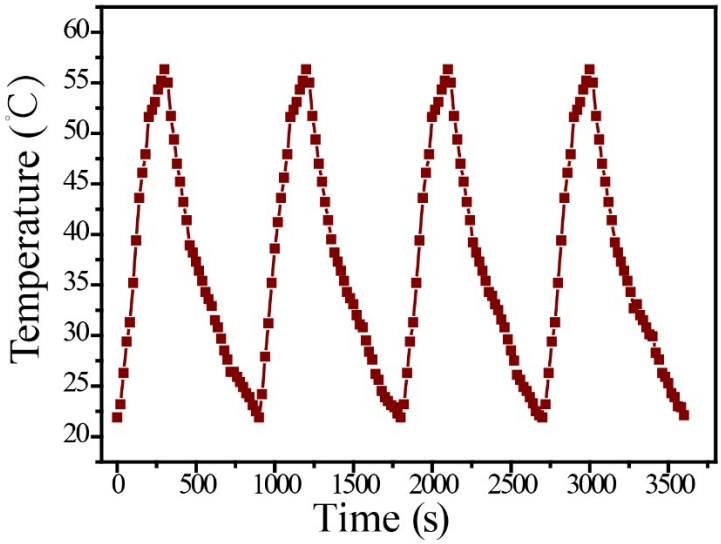

Figure S20. The photothermal conversion cycling of CMH aqueous solution (808 nm, 1 W cm^{-2}).

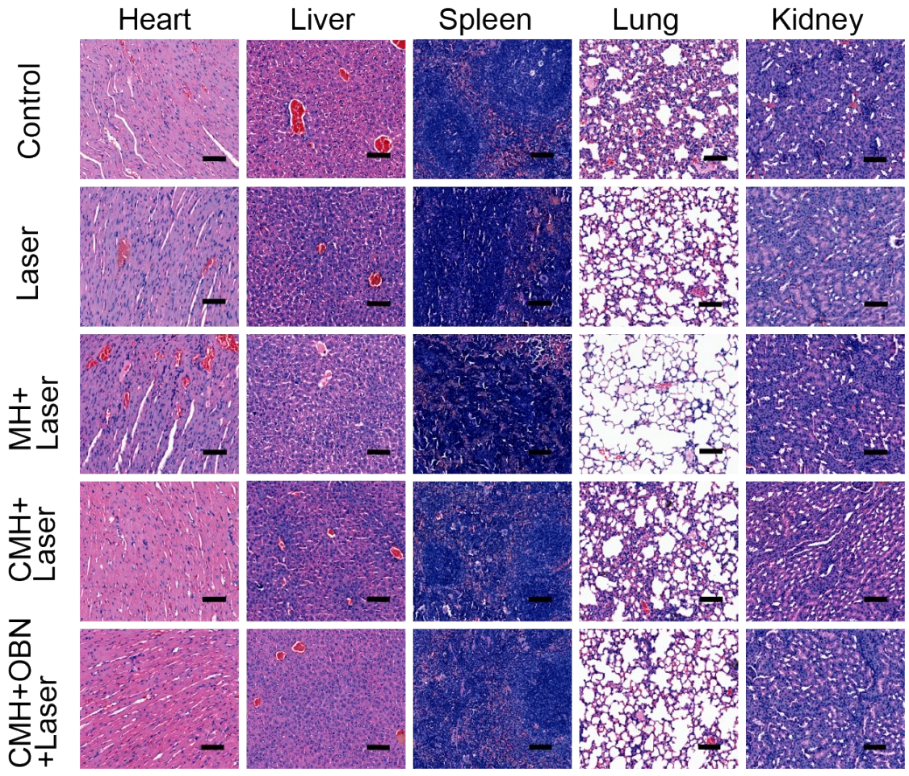

Figure S21. H&E staining of major organs of different groups on the 9th day (scale bar: 25 μm).

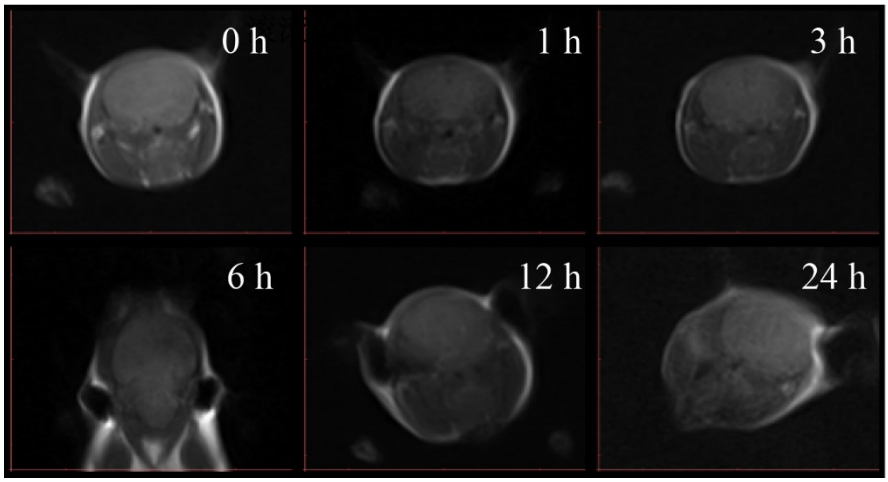

Figure S22. T1-weighted MR images of coronal plane of the brain of kunming mice irradiated for 5 min at different time points after intravenous injection of CMH NPs.

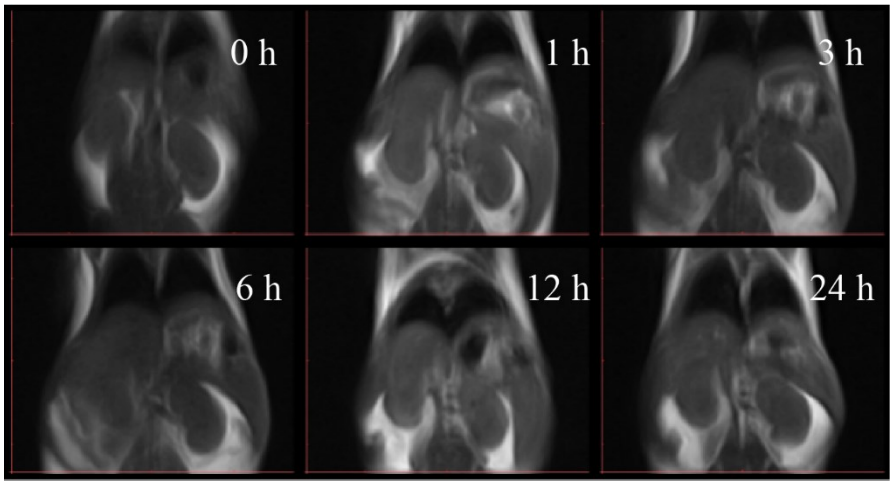

Figure S23. T1-weighted MR images of coronal plane of abdomen of kunming mice irradiated for 5 min at different time points after intravenous injection of CMH NPs.

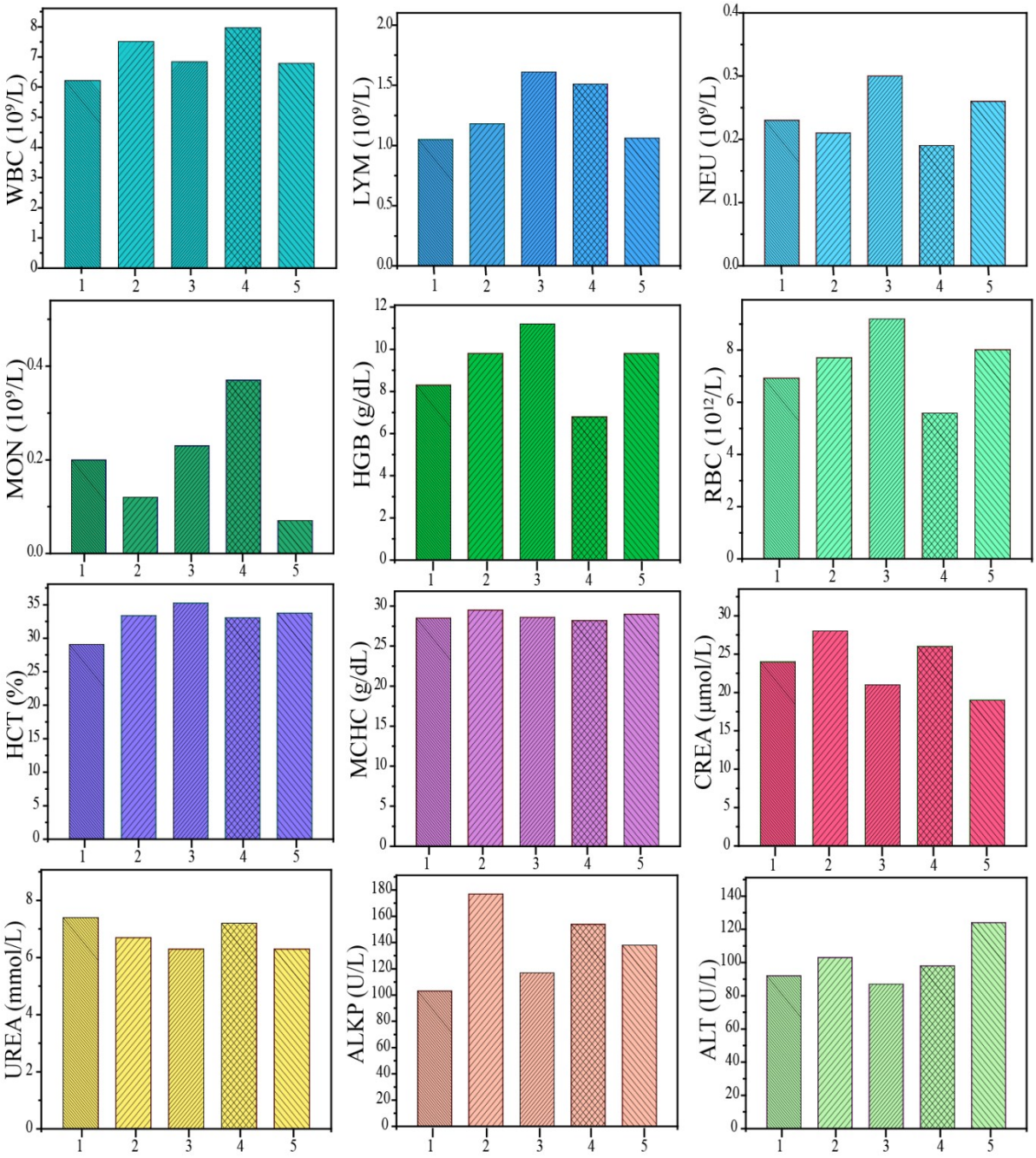

Figure S24. The serum biochemistry and complete blood panel analysis of Kunming mice.

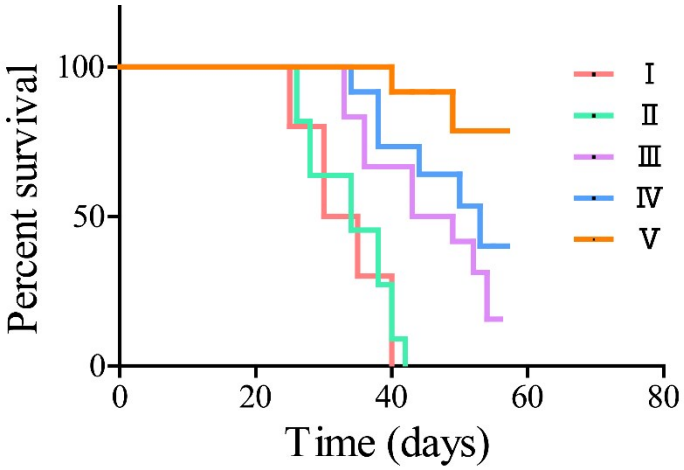

Figure S25. Survival curves of Kunming mice in different groups. Five groups: (Ⅰ) saline; (Ⅱ) saline + Laser; (Ⅲ) MH + Laser; (Ⅳ) CMH + Laser; (Ⅴ) CMH + OBN + Laser